DOI: 10.1021/ic101098v

Inorganic Chemistry
Article

Differences of pH-Dependent Mechanisms on Generation of Hydride Donors using Ru(II) Complexes Containing Geometric Isomers of NAD^+ Model Ligands: NMR and Radiolysis Studies in Aqueous Solution

Brian W. Cohen,[†] Dmitry E. Polyansky,[†] Ruifa Zong,[‡] Hui Zhou,[‡] Theany Ouk,[‡] Diane E. Cabelli,*[,†] Randolph P. Thummel,*[,‡] and Etsuko Fujita*[,†]

[†]*Chemistry Department, Brookhaven National Laboratory, Upton, New York 11973-5000, and* [‡]*Department of Chemistry, University of Houston, Houston, Texas 77204-5003*

Received May 31, 2010

The pH-dependent mechanism of the reduction of the nicotinamide adenine dinucleotide (NADH) model complex $[Ru(bpy)_2(\mathbf{5})]^{2+}$ (**5** = 3-(pyrid-2′-yl)-4-azaacridine) was compared to the mechanism of the previously studied geometric isomer $[Ru(bpy)_2(pbn)]^{2+}$ (pbn = 2-(pyrid-2′-yl)-1-azaacridine, previously referred to as 2-(pyrid-2′-yl)-benzo[*b*]-1,5-naphthyridine) in aqueous media. The exposure of $[Ru(bpy)_2(\mathbf{5})]^{2+}$ to $CO_2^{\bullet-}$ leads to the formation of the one-electron reduced species ($k = 4.4 \times 10^9\ M^{-1}\ s^{-1}$). At pH < 11.2, the one-electron reduced species can be protonated, $k = 2.6 \times 10^4\ s^{-1}$ in D_2O. Formation of a C−C bonded dimer is observed across the pH range of 5−13 ($k = 4.5 \times 10^8\ M^{-1}\ s^{-1}$). At pH < 11, two protonated radical species react to form a stable C−C bonded dimer. At pH > 11, dimerization of two one-electron reduced species is followed by disproportionation to one equivalent starting complex $[Ru(bpy)_2(\mathbf{5})]^{2+}$ and one equivalent $[Ru(bpy)_2(\mathbf{5}HH)]^{2+}$. The structural difference between $[Ru(bpy)_2(pbn)]^{2+}$ and $[Ru(bpy)_2(\mathbf{5})]^{2+}$ dictates the mechanism and product formation in aqueous medium. The exchange of the nitrogen and carbon atoms on the azaacridine ligands alters the accessibility of the dimerization reactive site, thereby changing the mechanism and the product formation for the reduction of the $[Ru(bpy)_2(\mathbf{5})]^{2+}$ compound.

Introduction

In an effort to mitigate the growing carbon dioxide (CO_2) concentration in the atmosphere, the chemical conversion of carbon dioxide into compounds that can be utilized as precursors to solar fuels has been extensively studied.[1,2] One of the very promising photochemical approaches is a succession of hydride-ion and proton-transfer reactions with CO_2 that is C-bonded to transition-metal catalytic centers.[3] Hydride donors should be cleanly generated photochemically, avoiding the coupling of carbon-centered radical intermediates, in order to implement this path. In biological systems NAD^+/NADH acts as a mediator for two electrons and a proton, equivalent to a hydride ion (H^-) to reduce CO_2. Increasing numbers of nicotinamide adenine dinucleotide (NADH) analogues, such as 9-substituted 10-methyl-9,10-dihydroacridine and 1-benzyl-1,4-dihydronicotinamide, have been examined for their photochemical and thermal reactivity.[4−35] Most of the reactions mediated with NADH models, however, are limited to stoichiometric reactions due in part to the facile

*Corresponding authors. E-mail: cabelli@bnl.gov (D.E.C.), thummel@uh.edu (R.P.T.), fujita@bnl.gov (E.F.).

(1) Basic Research Needs for Solar Energy Utilization: Report on the Basic Energy Science Workshop on Solar Energy Utilization, BES, US DOE, April 18−21, 2005, available at http://www.sc.doe.gov/bes/reports/files/SEU_rpt_print.pdf.
(2) Morris, A. J.; Meyer, G. J.; Fujita, E. *Acc. Chem. Res.* **2009**, *42*, 1983–1994.
(3) Doherty, M. D.; Grills, D. C.; Muckerman, J. T.; Polyansky, D. E.; Fujita, E. *Coord. Chem. Rev.* **2010**, ASAP, doi:10.1016/j.ccr.2009.12.013.
(4) Fukuzumi, S.; Kotani, H.; Lee, Y.-M.; Nam, W. *J. Am. Chem. Soc.* **2008**, *130*, 15134–15142.
(5) Ishikawa, M.; Fukuzumi, S. *J. Am. Chem. Soc.* **1990**, *112*, 8864–8870.
(6) Fukuzumi, S. In *Advances in Electon-Transfer Chemistry*; Mariano, P. S., Ed.; JAI Press Inc.: Greenwich, CT, 1992, p 67−175.
(7) Gebicki, J.; Marcinek, A.; Zielonka, J. *Acc. Chem. Res.* **2004**, *37*, 379–386.
(8) Fukuzumi, S.; Inada, O.; Suenobu, T. *J. Am. Chem. Soc.* **2003**, *125*, 4808–4816.
(9) Zhu, X. Q.; Yang, Y.; Zhang, M.; Cheng, J. P. *J. Am. Chem. Soc.* **2003**, *125*, 15298–15299.
(10) Nakanishi, I.; Ohkubo, K.; Fujita, S.; Fukuzumi, S.; Konishi, T.; Fujitsuka, M.; Ito, O.; Miyata, N. *J. Chem. Soc., Perkin Trans. 2* **2002**, 1829–1833.
(11) Fukuzumi, S.; Imahori, H.; Okamoto, K.; Yamada, H.; Fujitsuka, M.; Ito, O.; Guldi, D. M. *J. Phys. Chem. A* **2002**, *106*, 1903–1908.
(12) Zhu, X. Q.; Li, H. R.; Li, Q.; Ai, T.; Lu, J. Y.; Yang, Y.; Cheng, J. P. *Chem.—Eur. J.* **2003**, *9*, 871–880.
(13) Lu, Y.; Zhao, Y. X.; Handoo, K. L.; Parker, V. D. *Org. Biomol. Chem.* **2003**, *1*, 173–181.
(14) Gran, U. *Tetrahedron* **2003**, *59*, 4303–4308.
(15) Zhu, X. Q.; Cao, L.; Liu, Y.; Yang, Y.; Lu, J. Y.; Wang, J. S.; Cheng, J. P. *Chem.—Eur. J.* **2003**, *9*, 3937–3945.
(16) Mikata, Y.; Aida, S.; Yano, S. *Org. Lett.* **2004**, *6*, 2921–2924.
(17) Selvaraju, C.; Ramamurthy, P. *Chem.—Eur. J.* **2004**, *10*, 2253–2262.

 Published on Web 08/05/2010

Scheme 1. Ligands and Atom Numbering Sequence of NAD^+ Model Azaacridine Complexes

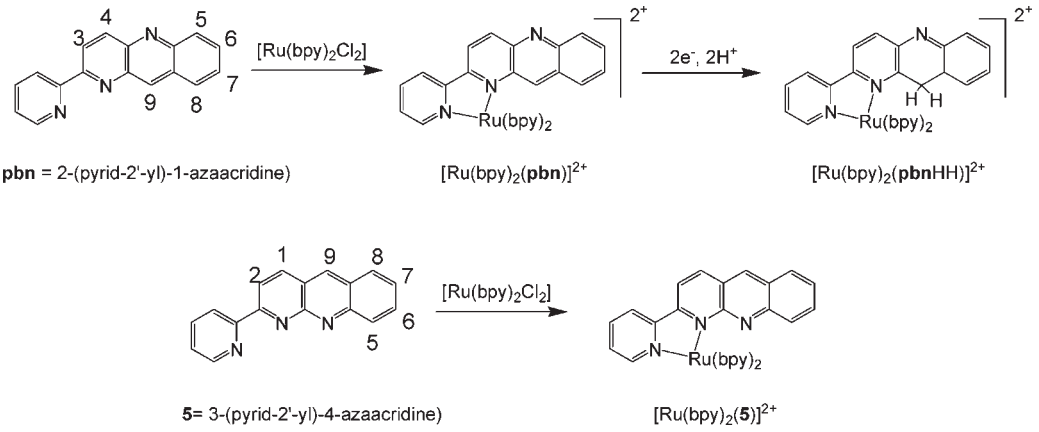

dimerization of the radical species (the $NAD^{\bullet}$ equivalent).[36−49] The introduction of transition metals into NADH analogues[50−52] imbues these systems with new characteristics, such as long-lived excited states, multiple oxidation states, catalytic activity, and efficient light absorption over a wide spectral range.

Previously, the electrocatalytic ability of a NADH model complex, $[Ru(bpy)_2(pbn)]^{2+}$ (pbn = 2-(pyrid-2′-yl)-1-azaacridine, previously referred to as 2-(pyrid-2′-yl)-benzo[*b*]-1,5-naphthyridine) for the reduction of acetone to isopropanol, with $[Ru(bpy)_2(pbnHH)]^{2+}$ (pbnHH = 2-(pyrid-2′-yl)-9,10-dihydro-1-azaacridine) as a key intermediate, has been reported (Scheme 1).[53] We demonstrated the photochemical generation of $[Ru(bpy)_2(pbnHH)]^{2+}$, which can be cleanly formed by the reductive quenching of the metal-to-ligand transfer (MLCT) excited state of $[Ru(bpy)_2(pbn)]^{2+}$ by triethylamine upon irradiation with visible light (< 600 nm).[51] A comprehensive mechanistic study, through steady and pulse radiolysis techniques, was previously undertaken to determine the pathways involved in the conversion of $[Ru(bpy)_2(pbn)]^{2+}$ into $[Ru(bpy)_2(pbnHH)]^{2+}$.[52]

For the $[Ru(bpy)_2(pbn)]^{2+}/[Ru(bpy)_2(pbnHH)]^{2+}$ couple, however, the ground-state hydride-donor ability and the excited-state reactivity for the catalytic hydrogenation of organic molecules has yet to be fully investigated. A major concern in the catalytic capacity of the pbnHH ligand is the accessibility of the hydride-donor reactive site on the C(9) carbon as both the X-ray structure and density functional theory (DFT) calculations have shown significant steric hindrance surrounding the site.[52,54] Therefore, the ability of hydride-acceptor molecules to interact with the hydride-donor site may be inhibited.

The inversion of the reactive site will potentially obviate the steric hindrance and allow for greater catalytic reactivity of the hydride-donor species if the C−C bonded dimer formation of the radical species can be avoided. To this end, the complex $[Ru(bpy)_2(\mathbf{5})]^{2+}$ (**5** = 3-(pyrid-2′-yl)-4-azaacridine,

(18) Ritter, S. C.; Eiblmaier, M.; Michlova, V.; Konig, B. *Tetrahedron* **2005**, *61*, 5241–5251.
(19) Buck, H. *Int. J. Quantum Chem.* **2005**, *101*, 389–395.
(20) Ishitani, O.; Inoue, N.; Koike, K.; Ibusuki, T. *J. Chem. Soc. Chem. Commun.* **1994**, 367–368.
(21) Kobayashi, A.; Sakamoto, K.; Ishitani, O. *Inorg. Chem. Commun.* **2005**, *8*, 365–367.
(22) Tanaka, M.; Ohkubo, K.; Fukuzumi, S. *J. Am. Chem. Soc.* **2006**, *128*, 12372–12373.
(23) Yuasa, J.; Yamada, S.; Fukuzumi, S. *J. Am. Chem. Soc.* **2006**, *128*, 14938–14948.
(24) Fang, X.-Q.; Xu, H.-J.; Jiang, H.; Liu, Y.-C.; Fu, Y.; Wu, Y.-D. *Tetrahedron Lett.* **2009**, *50*, 312–315.
(25) Yu Jin, J.; Yaeun, K.; Ah-Rim, H.; Yong-Min, L.; Hiroaki, K.; Shunichi, F.; Wonwoo, N. *Angew. Chem., Int. Ed.* **2008**, *47*, 7321–7324.
(26) Arunkumar, C.; Lee, Y. M.; Lee, J. Y.; Fukuzumi, S.; Nam, W. *Chem.—Eur. J.* **2009**, *15*, 11482–11489.
(27) Lee, J. Y.; Lee, Y. M.; Kotani, H.; Nam, W.; Fukuzumi, S. *J. Chem. Soc., Chem. Commun.* **2009**, 704–706.
(28) Fukuzumi, S.; Fujioka, N.; Kotani, H.; Ohkubo, K.; Lee, Y.-M.; Nam, W. *J. Am. Chem. Soc.* **2009**, *131*, 17127–17134.
(29) Yuasa, J.; Fukuzumi, S. *J. Phys. Org. Chem.* **2008**, *21*, 886–896.
(30) Yuasa, J.; Yamada, S.; Fukuzumi, S. *J. Am. Chem. Soc.* **2008**, *130*, 5808–5820.
(31) Koike, K.; Naito, S.; Sato, S.; Tamaki, Y.; Ishitani, O. *J. Photochem. Photobiol., A* **2009**, *207*, 109–114.
(32) Matsubara, Y.; Konno, H.; Kobayashi, A.; Ishitani, O. *Inorg. Chem.* **2009**, *48*, 10138–10145.
(33) Yuasa, J.; Yamada, S.; Fukushima, S. *Angew. Chem., Int. Ed.* **2008**, *47*, 1068–1071.
(34) Yuasa, J.; Fukuzumi, S. *J. Phys. Org. Chem.* **2008**, *21*, 886–896.
(35) Arunkumar, C.; Lee, Y.-M.; Lee, J. Y.; Fukuzumi, S.; Nam, W. *Chem.—Eur. J.* **2009**, *15*, 11482–11489.
(36) Hermolin, J.; Levin, M.; Ikegami, Y.; Sawayanagi, M.; Kosower, E. M. *J. Am. Chem. Soc.* **1981**, *103*, 4795–4800.
(37) Elving, P. J.; Bresnahan, W. T.; Moiroux, J.; Samec, Z. *J. Electroanal. Chem.* **1982**, *141*, 365–378.
(38) Hapiot, P.; Moiroux, J.; Saveant, J. M. *J. Am. Chem. Soc.* **1990**, *112*, 1337–1343.
(39) Hermolin, J.; Kosower, E. M. *J. Am. Chem. Soc.* **1981**, *103*, 4813–4816.
(40) Kosower, E. M. *Top. Curr. Chem.* **1983**, *112*, 117–162.
(41) Koper, N. W.; Jonker, S. A.; Verhoeven, J. W.; Van Dijk, C. *Recl. Trav. Chim. Pays-Bas* **1985**, *104*, 296.
(42) Neta, P.; Patterson, L. K. *J. Phys. Chem.* **1974**, *78*, 2211–2217.
(43) Kosower, E. M.; Teuerstein, A.; Burrows, H. D.; Swallow, A. J. *J. Am. Chem. Soc.* **1978**, *100*, 5185–5190.
(44) Moracci, F. M.; Liberatore, F.; Carelli, V.; Arnone, A.; Carelli, I.; Cardinali, M. E. *J. Org. Chem.* **1978**, *43*, 3420–3422.
(45) Ohnishi, Y.; Kitami, M. *Bull. Chem. Soc. Jpn.* **1979**, *52*, 2674–2677.
(46) Martens, F. M.; Verhoeven, J. W.; Varma, C.; Bergwerf, P. *J. Photochem. Photobiol., A* **1983**, *22*, 99–113.
(47) Bunting, J. W. *Bioorg. Chem.* **1991**, *19*, 456–491.
(48) Anne, A.; Hapiot, P.; Moiroux, J.; Saveant, J. M. *J. Electroanal. Chem.* **1992**, *331*, 959–970.
(49) Patz, M.; Kuwahara, Y.; Suenobu, T.; Fukuzumi, S. *Chem. Lett.* **1997**, 567–568.
(50) Kobayashi, A.; Konno, H.; Sakamoto, K.; Sekine, A.; Ohashi, Y.; Iida, M.; Ishitani, O. *Chem.—Eur. J.* **2005**, *11*, 4219–4226.
(51) Polyansky, D.; Cabelli, D.; Muckerman, J. T.; Fujita, E.; Koizumi, T.; Fukushima, T.; Wada, T.; Tanaka, K. *Angew. Chem., Int. Ed.* **2007**, *46*, 4169–4172.
(52) Polyansky, D. E.; Cabelli, D.; Muckerman, J. T.; Fukushima, T.; Tanaka, K.; Fujita, E. *Inorg. Chem.* **2008**, *47*, 3958–3968.
(53) Koizumi, T.; Tanaka, K. *Angew. Chem., Int. Ed.* **2005**, *44*, 5891–5894.
(54) Fukushima, T.; Fujita, E.; Muckerman, J. T.; Polyansky, D. E.; Wada, T.; Tanaka, K. *Inorg. Chem.* **2009**, *48*, 11510–11512.

Scheme 1) has been synthesized, and the mechanistic study of the reduction of $[Ru(bpy)_2(\mathbf{5})]^{2+}$ has been investigated. In this species, the reactive site is now open and more accessible toward hydride-acceptor compounds. This paper will describe the mechanism by which $[Ru(bpy)_2(\mathbf{5})]^{2+}$ is cleanly converted to $[Ru(bpy)_2(\mathbf{5HH})]^{2+}$ in aqueous solution (pH > 11) upon rapid addition of two protons and two electrons. This mechanism will then be contrasted with that shown previously for $[Ru(bpy)_2(pbn)]^{2+}$.

Experimental Section

Materials. Purification of acetronitrile (CH_3CN and CD_3CN) followed literature procedures,[55] and both compounds were subsequently stored in an inert atmosphere (Ar) glovebox. Aqueous solutions were prepared with water that had been passed through a Millipore ultrapurification system. Sodium formate was recrystallized (two times) from water. Blanket gases (N_2O and Ar) were UHP grade (99.999%). The 2-chloroquinoline-3-carbaldehyde (**2**),[56] 2-chloro-3-(1′,3′-dioxolan-2′-yl) quinoline (**3**),[57,58] 3-(pyrid-2′-yl)-4-azaacridine (**5**),[59] and $[Ru(bpy\text{-}d_8)_2]Cl_2\text{-}2H_2O$[60,61] were prepared according to modified literature procedures (Scheme S1, see Supporting Information). All other chemicals were of reagent grade and used without further purification.

2-Chloroquinoline-3-carbaldehyde (2). Dimethylformamide (DMF, 19.2 mL, 248 mmol) was cooled to 0 °C and $POCl_3$ (64.5 mL, 692 mmol) was added dropwise, producing a red solution. To the solution, acetanilide (**1**, 13.5 g, 100 mmol) was added. The mixture was refluxed overnight to give a dark-red solution. After cooling to room temperature, the reaction mixture was poured into 600 mL of ice to produce a yellow precipitate. The precipitate was collected, washed with water (200 mL), and dried (11.12 g, 58%), mp = 131−132 °C. ^{1}H NMR (500 MHz, $CDCl_3$) δ 10.55 (s, 1H), 8.74 (s, 1H), 8.06 (dd, 1H, J = 1.15, 8.59 Hz), 7.97 (dd, 1H, J = 1.15, 8.02 Hz), 7.88 (ddd, 1H, J = 1.72, 6.87, 8.73 Hz), 7.64 (ddd, 1H, J = 1.15, 6.87, 8.59 Hz); ^{13}C NMR (125 MHz, $CDCl_3$) δ 189.10, 150.07, 149.55, 140.24, 133.57, 129.69, 128.58, 128.10, 126.50, 126.35; IR (ATR, cm^{-1}) ν 1686 ($\nu_{C=O}$).

2-Chloro-3-(1′,3′-dioxolan-2′-yl)quinoline (3). A solution of 2-chloroquinoline-3-carbaldehyde (**2**, 3.00 g, 15.6 mmol), ethylene glycol (2.91 g, 47.0 mmol) and *p*-toluenesulfonic acid monohydrate (0.50 g) in benzene (80 mL) was heated at reflux under a Dean−Stark trap until thin-layer chromatography (TLC) (Al_2O_3, CH_2Cl_2/hexanes, 1:1) indicated completion of the reaction. The solution was cooled, and a saturated aqueous $NaHCO_3$ solution (50 mL) was added. The organic layer was washed with water (2 × 50 mL), dried over $MgSO_4$, and evaporated to afford **3** as a light-brown oil (3.61 g, 98%). A sample for spectroscopic analysis was purified by Kugelrohr distillation: ^{1}H NMR (500 MHz, $CDCl_3$) δ 8.28 (d, 1H, J = 1.72 Hz), 7.90 (d, 1H, J = 8.59 Hz), 7.72 (d, 1H, J = 8.02 Hz), 7.64−7.60 (m, 1 H), 7.46−7.42 (m, 1H), 6.12 (d, 1H, J = 2.29 Hz), 4.09−3.99 (m, 4H); ^{13}C NMR (125 MHz, $CDCl_3$) δ 148.91, 147.32, 136.41, 130.70, 129.17, 127.83, 127.77, 126.98, 126.46, 100.07, 65.25.

2-Aminoquinoline-3-carbaldehyde (4). A mixture of 2-chloro-3-(1′,3′-dioxolan-2′-yl)quinoline (**3**, 5.66 g, 24.0 mmol), K_2CO_3 (100 g, 724 mmol), and acetamide (120 g, 2.03 mol) was stirred mechanically at 200 °C for 4 h. After cooling, the mixture was treated with water (200 mL), and a mixture of $CHCl_3$−isopropanol (3:1, 3 × 60 mL). The combined organic phases were washed with brine (150 mL) and dried over Na_2SO_4. The solvents were evaporated to yield an oil (7.82 g). This crude product was mixed with THF (100 mL), H_2O (50 mL) and concentrated HCl (5 mL), refluxed for 45 min, and concentrated to produce a yellow precipitate which was filtered. The filtrate was extracted with $CHCl_3$ (3 × 30 mL), and the aqueous phase was basified with aqueous K_2CO_3 to produce a yellow precipitate. The precipitate was collected, washed with water, and dried (700 mg, 17%), mp 167−168 °C (lit.[62] mp = 197 °C): ^{1}H NMR (500 MHz, $CDCl_3$) δ 10.05 (s, 1 H), 8.36 (s, 1 H), 7.74 (dd, 1H, J = 1.72, 8.02 Hz), 7.70 (ddd, 1H, J = 1.44, 6.85, 8.31 Hz), 7.63 (dd, 1H, J = 1.15, 8.02 Hz), 7.29 (ddd, 1H, J = 1.15, 6.87, 8.02 Hz), 6.61 (br s, 2H); ^{13}C NMR (125 MHz, $CDCl_3$) δ 192.60, 155.37, 150.46, 148.28, 133.73, 129.20, 125.89, 123.07, 122.48, 117.28; IR (ATR, cm^{-1}) ν 3406 (ν_{NH_2}), 1676 ($\nu_{C=O}$).

3-(Pyrid-2′-yl)-4-azaacridine (5). A mixture of **4** (86 mg, 0.50 mmol), 2-acetylpyridine (150 mg, 1.24 mmol), EtOH (4 mL), and KOH (4 mg) was refluxed overnight. The solvent was removed, and red residue was subjected to chromatography on neutral alumina eluting with CH_2Cl_2 to afford a crude sample of **5** (90 mg, 70%). Washing this material with diethyl ether gave a purified sample, mp 195 °C (lit.[59] mp = 201 °C): ^{1}H NMR (500 MHz, $CDCl_3$) δ 9.00 (d, 1H, J = 8.02 Hz), 8.78 (s, 1H), 8.75 (dd, 1H, J = 1.15, 5.73 Hz), 8.73 (d, 1H, J = 8.59 Hz), 8.44 (d, 1H, J = 8.59 Hz), 8.39 (d, 1H, J = 8.02 Hz), 8.00 (d, 1H, J = 8.59 Hz), 7.90 (dt, 1H, J = 1.72, 7.73 Hz), 7.82 (ddd, 1H, J = 1.15, 6.45, 9.31 Hz), 7.57 (ddd, 1H, J = 1.15, 6.87, 8.59 Hz), 7.40 (ddd, 1H, J = 1.15, 4.58, 7.45 Hz); ^{13}C NMR (125 MHz, $CDCl_3$) δ 161.28, 155.32, 154.43, 150.97, 149.04, 137.96, 137.44, 136.97, 131.23, 129.98, 127.92, 127.03, 126.51, 124.92, 122.99, 121.09, 119.34.

$[Ru(bpy)_2(\mathbf{5})](PF_6)_2$. A mixture of $[Ru(bpy)_2Cl_2]\text{-}2H_2O$ (157 mg, 0.30 mmol) and **5** (78 mg, 0.30 mmol) in EtOH (15 mL) and water (5 mL) was refluxed for 3 d. The resulting solution was concentrated to about 5 mL, and NH_4PF_6 (430 mg, 2.64 mmol) was added to precipitate the complex. The crude product was purified by column chromatography on neutral alumina eluting with CH_2Cl_2 and CH_2Cl_2/CH_3CN (3:2). The complex was obtained from the latter fractions as dark-red crystals (253 mg, 88%): ^{1}H NMR (500 MHz, CD_3CN): δ 9.14 (s, 1H), 8.84 (d, 1H, J = 8.6 Hz), 8.80 (d, 1H, J = 9.2 Hz), 8.61 (d, 1H, J = 9.2 Hz), 8.53−8.50 (m, 2H), 8.44 (d, 1H, J = 8.0 Hz), 8.33 (d, 1H, J = 8.6 Hz), 8.16 (dt, 1H, J = 1.4, 7.9 Hz), 8.13−8.05 (m, 3H), 8.01 (dt, 1H, J = 1.4, 7.9 Hz), 7.92 (d, 1H, J = 5.7 Hz), 7.88 (dt, 1H, J = 1.4, 7.9 Hz), 7.83 (d, 1H, J = 5.7 Hz), 7.78 (d, 1H, J = 5.7 Hz), 7.72 (ddd, 1H, J = 1.4, 6.6, 8.9 Hz), 7.68 (d, 1H, J = 5.7 Hz), 7.62 (ddd, 1H, J = 1.2, 6.9, 8.0 Hz), 7.59 (d, 1H, J = 5.7 Hz), 7.50−7.46 (m, 2H), 7.40 (ddd, 1H, J = 1.2, 5.6, 7.6 Hz), 7.26 (ddd, 1H, J = 1.2, 5.7, 9.2 Hz), 7.20 (ddd, 1H, J = 1.2, 5.7, 7.5 Hz), 6.78 (dd, 1H, J = 8.0 Hz). ^{1}H NMR (400 MHz, D_2O): δ 9.07 (s, 1H), 8.85 (d, 1H, J = 8.0 Hz), 8.76 (d, 1H, J = 8.8 Hz), 8.63 (d, 1H, J = 8.8 Hz), 8.54−8.50 (m, 2H), 8.48 (d, 1H, J = 8.4 Hz), 8.34 (d, 1H, J = 8.0 Hz), 8.14−8.02 (m, 4H), 7.99−7.95 (m, 2H), 7.91 (d, 1H, J = 5.2 Hz), 7.86−7.79 (m, 3H), 7.71−7.68 (m, 2H), 7.57 (t, 1H, J = 6.8 Hz), 7.44−7.40 (m, 2H), 7.35 (t, 1H, J = 6.8 Hz), 7.21−7.14 (m, 2H), 7.75 (d, 1H, J = 9.2). UV−vis in H_2O, λ_{max}, nm (ε, mM^{-1} cm^{-1}): 236 (40.2), 254 (27.0), 288 (73.6), 352 (19.5), 374 (16.7), 392 (12.8), 446 (7.6), 552 (7.1). UV−vis in CH_3CN, λ_{max}, nm (ε, mM^{-1} cm^{-1}): 236 (45.3), 254 (33.6), 288 (88.5), 352 (22.9), 374 (18.9), 392 (14.5), 446 (9.1), 552 (8.5). MS (MALDI-TOF): m/z 816.12 $[M - PF_6]^+$, 671.20 $[M - 2PF_6]^+$. ESI-MS: m/z = 335.8 $[M - 2PF_6]^{2+}$. Anal. calcd for

(55) Amarego, W., L.F.; Chai, C., L.L. *Purification of Laboratory Chemicals*; 5th ed.; Elsevier: Oxford, U.K., 2003.
(56) Meth-Cohn, O.; Narine, B.; Tarnowski, B. *Tetrahedron Lett*. **1979**, *20*, 3111–3114.
(57) Nyerges, M.; Pinter, A.; Viranyi, A.; Blasko, G.; Toke, L. *Tetrahedron* **2005**, *61*, 8199–8205.
(58) Farghaly, A. M.; Habib, N. S.; Khalil, M. A.; El-Sayed, O. A.; Bistawroos, A. E. *Arch. Pharm*. **1990**, *323*, 247–251.
(59) Godard, A.; Queguiner, G. *J. Heterocyclic Chem*. **1982**, *19*, 1289–1296.
(60) Chirayil, S.; Thummel, R. P. *Inorg. Chem*. **1989**, *28*, 812–813.
(61) Keyes, T. E.; Weldon, F.; Muller, E.; Pechy, P.; Gratzel, M.; Vos, J. G. *J. Chem. Soc., Dalton Trans*. **1995**, 2705–2706.
(62) Godard, A.; Queguiner, G. *J. Heterocycl. Chem*. **1980**, *17*, 465–473.

$C_{37}H_{27}F_{12}N_7P_2Ru \cdot 0.5H_2O$: C, 45.83; H, 2.91; N, 10.11. Found: C, 45.72; H, 2.94; N, 9.87.

[Ru(bpy-d_8)$_2$(5)](PF$_6$)$_2$. A mixture of [Ru(bpy-d_8)$_2$Cl$_2$]-2H$_2$O (81 mg, 0.15 mmol) and **5** (40 mg, 0.15 mmol) was refluxed in EtOH (10 mL) and water (5 mL) for 60 h. The complex was precipitated by the addition of NH_4PF_6 (162 mg, 1.0 mmol). The precipitate was collected, washed with water, and purified on a neutral alumina column eluting with CH_2Cl_2 with 0−50% acetone. Recrystallization from acetone−water gave crystals of the complex (110 mg, 73%): ^{1}H NMR (500 MHz, CD_3CN) δ 9.14 (s, 1H, **5**-H9), 8.85 (d, 1H, J = 8.2 Hz, **5**-py-H3), 8.81 (d, 1H, J = 8.7 Hz, **5**-H1 or 2), 8.63 (d, 1H, J = 8.7 Hz, **5**-H1 or H2), 8.16 (dt, 1H, J = 1.4, 8.7 Hz, **5**-py-H4), 8.11 (d, 1H, J = 8.2 Hz, **5**-H8), 7.84 (dd, 1H, J = 0.9, 5.6 Hz, **5**-py-H6), 7.73 (ddd, 1H, J = 1.6, 6.9, 8.7 Hz, **5**-H6), 7.62 (ddd, 1H, J = 0.9, 6.6, 9.4 Hz, **5**-H7), 7.49 (ddd, 1H, J = 1.2, 5.5, 8.7 Hz, **5**-py-H5), 6.78 (d, 1H, J = 8.2 Hz, **5**-H5). ^{1}H NMR (400 MHz, D_2O): δ 9.13 (s, 1H, **5**-H9), 8.88 (d, 1H, J = 8.0 Hz, **5**-py-H3), 8.81 (d, 1H, J = 8.8 Hz, **5**-H2), 8.67 (d, 1H, J = 8.4 Hz, **5**-H1), 8.16 (t, 1H, J = 8.0 Hz, **5**-py-H4), 8.11 (d, 1H, J = 5.2, **5**-H8), 7.94 (d, 1H, J = 5.2, **5**-py-H6), 7.74 (t, 1H, J = 8.0 Hz, **5**-H6), 7.63 (t, 1H, J = 7.5 Hz, **5**-H7), 7.46 (t, 1H, J = 6.5 Hz, **5**-py-H5), 6.79 (d, 1H, J = 8.8 Hz, **5**-H5). ^{1}H NMR (400 MHz, 1:1 D_2O/CD_3OD): δ 9.21 (s, 1H, **5**-H9), 8.99 (d, 1H, J = 8.1 Hz, **5**-py-H3), 8.90 (d, 1H, J = 9.2 Hz, **5**-H2), 8.76 (d, 1H, J = 9.2 Hz, **5**-H1), 8.23 (td, 1H, J = 7.4, 1.2 Hz, **5**-py-H4), 8.14 (d, 1H, J = 8.0, **5**-H8), 7.92 (d, 1H, J = 4.8, **5**-py-H6), 7.75 (td, 1H, J = 6.8, 1.6 Hz, **5**-H6), 7.65 (t, 1H, J = 7.4, 1.2 Hz, **5**-H7), 7.55 (t, 1H, J = 6.6, 1.2 Hz, **5**-py-H5), 6.75 (d, 1H, J = 8.4 Hz, **5**-H5). ^{13}C NMR (125 MHz, CD_3CN) δ 164.6, 159.6, 159.2, 158.4, 158.3, 158.0, 156.5, 153.6, 151.4, 141.5, 141.3, 138.8, 134.2, 129.8, 129.7, 129.7, 129.2, 129.0, 129.0, 123.4, 120.4. ESI-MS: m/z 343.9 $[M - 2PF_6]^{2+}$.

[Ru(bpy-d_8)$_2$(5HH)](PF$_6$)$_2$. To a pH 13 aqueous solution (10 mL) of [Ru(bpy-d_8)$_2$(**5**)](PF$_6$)$_2$ (5.0 mg, 5.1 μmol), $Na_2S_2O_4$ (2.2 mg, 12.6 μmol) was added under an argon atmosphere using standard glovebox techniques. The reaction mixture was allowed to stir for 14 h, during which time the color changed from red to dark yellow-orange. Afterward, the reaction mixture was layered onto a pH 13 saturated aqueous solution of NH_4PF_6. An orange-brown precipitate formed and was collected on a sintered glass frit. The residue was dissolved in CH_3CN (2 mL) and collected. The CH_3CN was removed under high vacuum, and the complex was dried overnight at room temperature: ^{1}H NMR (400 MHz, CD_3CN): δ 8.39 (d, 1H, J = 8.0 Hz, **5**-py-H3), 7.99 (t, 1H, **5**-py-H4), 7.94 (d, 1H, J = 7.6 Hz, **5**-H2), 7.69 (d, 1H, J = 8.0 Hz, **5**-H1), 7.45 (d, 1H, J = 5.6 Hz, **5**-py-H6), 7.26 (t, 1H, **5**-py-H5), 7.05 (d, 1H, J = 4.8 Hz, **5**-H8), 6.87 (overlapping m, 2H, **5**-H6,7), 6.70 (s, 1H, **5**-NH10), 5.26 (d, 1H, J = 7.2 Hz, **5**-H5), 4.23 (d, 1H, J = 22 Hz, **5**-H9), 4.10 (d, 1H, J = 21 Hz, **5**-H9). ^{1}H NMR (400 MHz, 1:1 D_2O/CD_3OD): δ 8.48 (d, 1H, J = 8.0 Hz, **5**-py-H3), 8.05 (d, 1H, J = 8.0 Hz, **5**-H2), 8.02 (t, 1H, **5**-py-H4), 7.76 (d, 1H, J = 8.0 Hz, **5**-H1), 7.49 (d, 1H, J = 5.6 Hz, **5**-py-H6), 7.28 (t, 1H, **5**-py-H5), 7.06 (m, 1H, **5**-H8), 6.87 (overlapping m, 2H, **5**-H7,8), 5.18 (m, 1H, **5**-H5), 4.24 (d, 1H, J = 22 Hz, **5**-H9), 4.07 (d, 1H, J = 21 Hz, **5**-H9). ESI-MS: m/z 688.4 $[M - (H^+, 2PF_6)]^+$.

[Ru(bpy-d_8)$_2$(5H)]$_2$(PF$_6$)$_4$. To a pH 7 D_2O solution (8 mL) of [Ru(bpy-d_8)$_2$(**5**)](PF$_6$)$_2$ (4.2 mg, 4.3 μmol), $Na_2S_2O_4$ (3.0 mg, 17.2 μmol) was added under an argon atmosphere using standard glovebox techniques. The reaction mixture was allowed to stir for 3 h, during which time the color changed from red to orange. To obtain the NMR spectrum in a 1:1 D_2O/CD_3OD solution, the reaction mixture was concentrated to 0.5 mL under vacuum, upon which 0.5 mL CD_3OD was added to the solution. Two isomers seem to exist with the approximate ratio of 2:1. The major isomer has the following NMR signals: ^{1}H NMR (400 MHz, 1:1 D_2O/CD_3OD): δ 8.53 (d, 1H, J = 8.4 Hz, **5**-py-H3), 8.10 (d, 1H, J = 8.0 Hz, **5**-H2), 8.04 (td, 1H, J = 7.4, 1.2 Hz, **5**-py-H4), 7.66 (d, 1H, J = 8.8 Hz, **5**-H1), 7.47 (d, 1H, J = 5.2 Hz, **5**-py-H6), 7.30 (t, 1H, **5**-py-H5), 7.12 (m, 1H, **5**-H8), 6.92 (overlapping m, 2H, **5**-H6,7), 5.06 (m, 1H, **5**-H5), 4.29 (s, 1H, **5**-H9). ESI-MS: m/z 687.3 $[M - (2H^+, 4PF_6)]^{2+}$.

Spectroscopic Measurements. NMR spectra were measured on a Bruker UltraShield 400 MHz spectrometer or on a JEOL ECX-500 spectrometer operating at 500 and 125 MHz for ^{1}H and ^{13}C, respectively. Chemical shifts were reported in parts per million (ppm) referenced to the residual solvent peaks for ^{1}H and ^{13}C. UV−vis-NIR spectroscopy was measured on either a Hewlett-Packard 8452A diode-array spectrophotometer, a Varian 5 or 500 CARY spectrophotometer, or an Agilent 8453 diode-array spectrophotometer. Photochemical irradiations were performed with a 420 nm cutoff filter from a 75 W lamp. Melting points were determined with a Thomas-Hoover capillary melting-point apparatus and are uncorrected. Infrared spectra were recorded with a Thermo Nicolet AVATAR 370 FT-IR spectrometer.

Electrochemical Measurements. Electrochemical measurements of [Ru(bpy)$_2$(**5**)]$^{2+}$ were conducted with a BAS 100b electrochemical analyzer from Bioanalytical Systems. For electrochemical measurements in water, a stationary mercury drop electrode (SMDE), a silver chloride (Ag/AgCl) electrode, and a platinum wire were used as the working, reference, and counter electrodes, respectively. The solutions contained [Ru(bpy)$_2$(**5**)]$^{2+}$ (1 mM) with 100 mM sodium triflate and sodium phosphate (5 mM or 10 mM) as an electrolyte and a buffer, respectively, were used between a pH of 3 and 10.

Pulse Radiolysis. Pulse radiolysis studies were carried out using the BNL 2 MeV Van de Graaff accelerator using electron pulses (pulse width 40−500 ns) that led to irradiation doses of 100−1000 rad (ca. 0.5−5 μM primary radicals) generated in water. A thiocyanate solution (0.01 M KSCN, 0.026 M N_2O) was used for dosimetry taking $G((SCN)_2^{\bullet-})$ = 6.13 (G = number of species formed per 100 eV of energy absorbed by the solution) and $\varepsilon_{472\ nm} = 7590 \pm 230$. The optical path of the cell was 2 cm. Typical measurements were carried out in N_2O saturated solutions of either H_2O or D_2O with 10 mM phosphate buffer, 10 mM sodium formate, and 30−60 μM [Ru(bpy)$_2$(**5**)]$^{2+}$ at 25 °C. Experiments to determine a general acid effect were carried out on a solution between 5−20 mM sodium formate and 0−20 mM phosphate buffer, where 1.0 M Na_2SO_4 was used to keep the ionic strength constant. Under these conditions, the conversion of the primary radicals to the carbon dioxide anion radical ($CO_2^{\bullet-}$) was complete by the first microsecond. Quoted rate constants have an error of ca. 15%. All rates measured in the pulse radiolysis studies are averages of at least three measurements. The pH of the solution was adjusted by addition of $NaOH/H_2SO_4$ or NaOD/DCl for H_2O and D_2O, respectively.

Radiolysis of aqueous solutions produces $^{\bullet}$OH, e_{aq}^-, and H$^{\bullet}$ with G values of 2.7, 2.6, and 0.6, respectively ($H_2O \rightarrow {}^{\bullet}OH$, e_{aq}^-, H$^{\bullet}$, H_2, H_2O_2).[63] In a nitrous oxide saturated aqueous solution, the hydrated electron is converted to $^{\bullet}$OH ($e_{aq}^- + N_2O + H_2O \rightarrow OH^{\bullet} + OH^- + N_2$). Radiolysis of a nitrous oxide saturated aqueous solution containing HCO_2^- leads to exclusive production of the carbon dioxide anion radical $CO_2^{\bullet-}$, since both OH$^{\bullet}$ and H$^{\bullet}$ react with HCO_2^- ($OH^{\bullet}/H^{\bullet} + HCO_2^- \rightarrow H_2O/H_2 + CO_2^{\bullet-}$). $CO_2^{\bullet-}$ is a strong reducing agent ($E = -1.90$ V)[64] that undergoes protonation only under very acidic conditions ($pK_a = -0.2$).[65]

^{60}Co Gamma Radiolysis. Steady-state radiolysis studies were carried out using the BNL 650 Ci ^{60}Co γ-ray source. The chemistry that ensues is identical to that in pulse radiolysis since, in water, both γ-rays and electrons produce the same yield

(63) Buxton, G. V.; Greenstock, C. L.; Helman, W. P.; Ross, A. B. *J. Phys. Chem. Ref. Data* **1988**, *17*, 513–886.
(64) Schwarz, H. A.; Dodson, R. W. *J. Phys. Chem.* **1989**, *93*, 409–414.
(65) Kawanishi, Y.; Kitamura, N.; Tazuke, S. *Inorg. Chem.* **1989**, *28*, 2968–2975.

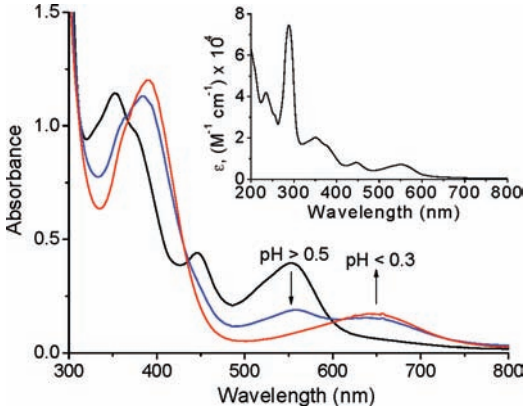

Figure 1. The pH-dependent UV−vis spectra of stepwise protonation of $[Ru(bpy)_2(\mathbf{5})]^{2+}$ (black) to $[Ru(bpy)_2(\mathbf{5H})]^{3+}$ (red) in H_2O. Inset: UV−vis spectrum of $[Ru(bpy)_2(\mathbf{5})]^{2+}$ in H_2O.

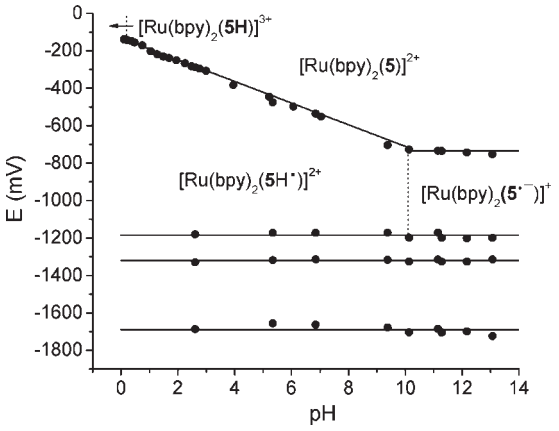

Figure 2. Reduction potentials of $[Ru(bpy)_2(\mathbf{5})]^{2+}$ in H_2O with 5 mM of phosphate buffer between a pH of 3−10.

of primary species. Here, a continuous flux of radicals is produced at a low steady-state concentration, with a production rate of ca. 0.4 μM $CO_2^{\bullet-}$/s in N_2O-saturated solutions containing HCO_2^-.

Results

Ground-State Properties of $[Ru(bpy)_2(\mathbf{5})]^{2+}$. The UV−vis absorption spectrum of an aqueous solution of $[Ru(bpy)_2(\mathbf{5})]^{2+}$ at a neutral pH (Figure 1, inset) shows typical transitions for mixed-ligand complexes with two MLCT transitions centered at 552 and 446 nm as well as $\pi-\pi^*$ transitions centered at 288 nm (**5** and bpy) and 380 nm (**5**). The N(10) atom of the azaacridine moiety can be protonated with a strong acid to produce $[Ru(bpy)_2(\mathbf{5H})]^{3+}$, which has a $pK_a \approx 0.2$. The UV−vis spectrum of the protonated compound exhibits a decrease in intensity of the transitions between 352 and 552 nm as well as the appearance of transitions at 388 and 646 nm (Figure 1).

The electrochemistry of $[Ru(bpy)_2(\mathbf{5})]^{2+}$ in aqueous solution shows four quasireversible reduction waves. The first reduction potential, representing the $[Ru(bpy)_2(\mathbf{5})]^{2+}/[Ru(bpy)_2(\mathbf{5}^{\bullet-})]^{+}$ redox couple, is pH-dependent over the pH range of 0.2−10 (Figure 2). The slope of the wave is 59 mV/pH, which is indicative of the proton-coupled nature of the redox reaction to produce the neutral ligand−radical complex $[Ru(bpy)_2(\mathbf{5H}^{\bullet})]^{2+}$. The pH-independent potentials at −1.32 and −1.69 V are due

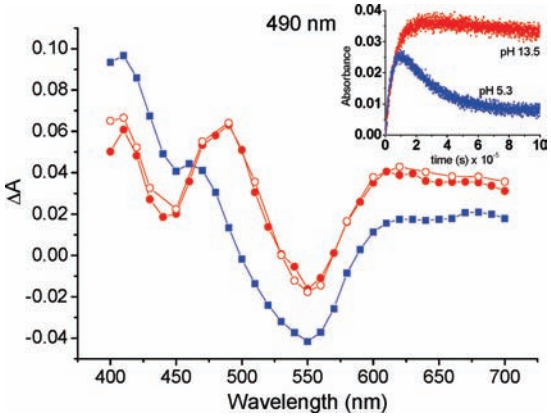

Figure 3. Pulse radiolysis of $[Ru(bpy)_2(\mathbf{5})]^{2+}$: Differential absorption spectra in D_2O at a pH of 5.3 and 13.5 (radical anion at pH 5.3, 7 μs after pulse: circles (●); radical anion at pH 13.5, 7 μs after pulse: open circles (○); and protonated radical at pH 5.3, 100 μs after pulse: squares (■)). The solutions were buffered with 10 mM phosphate buffer. Inset: Absorbance trace at pH 5.3 and 13.5 measured at 490 nm in D_2O.

to the $(bpy)_2/(bpy, bpy^{\bullet-})$ and $(bpy^{\bullet-}, bpy)/(bpy^{\bullet-}, bpy^{\bullet-})$ redox couples, respectively. The pH-independent potential at −1.19 V may correspond to the reduction of the C−C bonded dimer, $[Ru(bpy)_2(\mathbf{5H})]_2^{4+}$, which forms rapidly (see the Pulse Radiolysis Section). In CH_3CN, pH-independent potentials at −0.75, −1.34, and −1.62 V are observed.

Pulse Radiolysis. On the 100 μs time scale, the exposure of aqueous solutions of $[Ru(bpy)_2(\mathbf{5})]^{2+}$ to $CO_2^{\bullet-}$ that were generated on submicrosecond time scales initially leads to the formation of a single transient absorption spectrum between the pH range of 5.3−13.5 (Figure 3). At pH 13.5, the transient absorption spectrum does not degrade on the 100 μs time scale. At pH 5.3, however, a subsequent transformation of the species is observed (Figure 3, inset).

At a pH of 5.3, the rates of the initial and subsequent reactions were monitored, in both H_2O and D_2O, to determine a kinetic isotope effect (KIE) as well as to determine the individual rates of the first and secondary reactions. The initial reaction between $CO_2^{\bullet-}$ and $[Ru(bpy)_2(\mathbf{5})]^{2+}$ (eq 1) was monitored by the formation of the reduced species $[Ru(bpy)_2(\mathbf{5}^{\bullet-})]^{+}$ at 490 nm. The observed difference spectra can be corrected for the loss of parent compound, assuming a 1:1 stoichiometry as seen in eq 1.

$$[Ru(bpy)_2(\mathbf{5})]^{2+} + CO_2^{\bullet-} \rightarrow [Ru(bpy)_2(\mathbf{5}^{\bullet-})]^{+} + CO_2 \quad (1)$$

The absorption spectrum of the transient species is shown in Figure 4.

The UV−vis spectrum of the initially observed species exhibits absorption bands around 490 and 600 nm, consistent with those of the one-electron reduced species formed by Na−Hg reduction or reductive quenching of the excited-state of $[Ru(bpy)_2(\mathbf{5})]^{2+}$.[66] A small decrease in the rate of reaction between $CO_2^{\bullet-}$ and $[Ru(bpy)_2(\mathbf{5})]^{2+}$ is observed at pH < 11.2. This is consistent with a slower rate of reaction in a solution with a lower ionic strength. A

(66) Cohen, B. W.; Polyansky, D. E.; Zong, R.; Cabelli, D.; Muckerman, J. T.; Thummel, R. P.; Fujita, E., manuscript in prep.

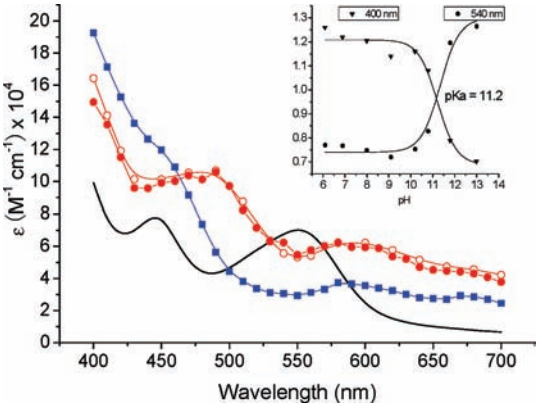

Figure 4. UV−vis absorbance spectra in D_2O at a pH of 5.3 and 13.5, corrected for parent compound loss assuming stoichiometric loss of $[Ru(bpy)_2(\mathbf{5})]^{2+}$ and generation of transient species (radical anion at a pH of 5.3, 7 μs after pulse: circles (●); radical anion at pH 13.5, 7 μs after pulse: open circles (○); protonated radical at pH 5.3, 100 μs after pulse: squares (■); and $[Ru(bpy)_2(\mathbf{5})]^{2+}$: solid line (—)). Inset: Titration curves obtained by plotting absorbances measured immediately after exposure of $[Ru(bpy)_2(\mathbf{5})]^{2+}$ aqueous solutions to $CO_2^{\bullet-}$ radical vs pH at 400 (triangles, ▲) and 540 nm (dots, ···).

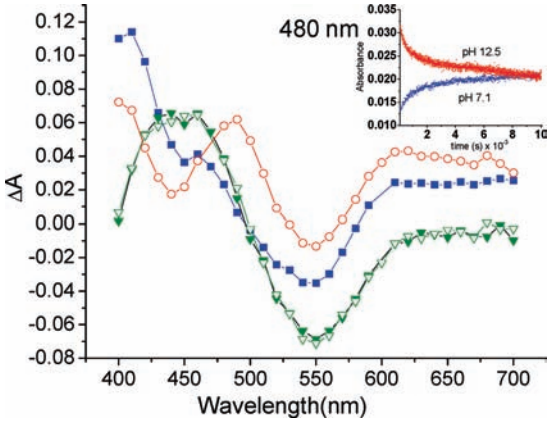

Figure 5. Pulse radiolysis of $[Ru(bpy)_2(\mathbf{5})]^{2+}$: differential absorption spectra in H_2O at a pH of 7.1 and 12.5 (protonated radical at pH 7.1, 100 μs after pulse: squares (■); radical anion at pH 12.5, 100 μs after pulse: open circles (○); dimer at pH 7.1, 10 ms after pulse: triangles (▲); and dimer at pH 12.5, 10 ms after pulse: open triangles, (△). The solutions were buffered with 10 mM phosphate buffer. Inset: Absorbance trace at pH of 7.1 and 12.5 measured at 480 nm in H_2O.

KIE of 1.2 is observed between the rates of reaction between $CO_2^{\bullet-}$ and $[Ru(bpy)_2(\mathbf{5})]^{2+}$ at both a pH of 7.3 and 12.5 in H_2O and D_2O. The linear plots of the observed rate constants for the formation of $[Ru(bpy)_2(\mathbf{5}^{\bullet-})]^{+}$ as a function of $[Ru(bpy)_2(\mathbf{5})]^{2+}$ concentration gives $k_1 = 4.4 \times 10^9$ in H_2O and 3.8×10^9 M^{-1} s^{-1} in D_2O (Supporting Information, Figure S1).

By measuring the pH-dependent change in the absorption spectrum, on the 100 μs time scale (Figure 4, inset), a pK_a value of 11.2 was determined for the secondary reaction. This pK_a value is consistent with the one obtained in electrochemical experiments. Earlier work on similar ruthenium-containing complexes[52,67−70] suggests that this pK_a is indicative of the protonation of the nitrogen on the azaacridine ligand of the reduced anionic radical species. In H_2O, the limit of solubility of $[Ru(bpy)_2(\mathbf{5})]^{2+}$ leads to a first-order rate of formation of $[Ru(bpy)_2(\mathbf{5}^{\bullet-})]^{+}$ that is indistinguishable from the rate of protonation of the radical. In D_2O, however, the rate of protonation of $[Ru(bpy)_2(\mathbf{5}^{\bullet-})]^{+}$ is slow enough to measure, $k_{2b} = 2.6 \times 10^4$ s^{-1}. For the protonation of $[Ru(bpy)_2(\mathbf{5}^{\bullet-})]^{+}$, the proton source is either H_2O or D_2O dependent on the solvent in which the experiment is performed. To confirm the origin of the source of protons, the concentration of phosphate was varied between 0−20 mM, while the concentration of formate was varied between 5−20 mM. Verification of the proton source is established by the independence of the rate of protonation in relation to the concentrations of the general acid donor. On the 100 μs time scale, over the pH range of 5.3−13.5, the initial transient species formed is the radical anionic species $[Ru(bpy)_2(\mathbf{5}^{\bullet-})]^{+}$. At pH < 11.2 the radical anion is then protonated by water to form $[Ru(bpy)_2(\mathbf{5H}^{\bullet})]^{2+}$ (eqs 2a and 2b), as shown in the change in the difference and absorption spectra (Figures 3 and 4, respectively).

$$[Ru(bpy)_2(\mathbf{5}^{\cdot-})]^{+} + H^{+} \rightarrow [Ru(bpy)_2(\mathbf{5H}^{\cdot})]^{2+} \quad (2a)$$

$$[Ru(bpy)_2(\mathbf{5}^{\cdot-})]^{+} + D^{+} \rightarrow [Ru(bpy)_2(\mathbf{5D}^{\cdot})]^{2+} \quad (2b)$$

On the 10 ms time scale, following the formation of the radical anion $[Ru(bpy)_2(\mathbf{5}^{\bullet-})]^{+}$ or the protonated radical $[Ru(bpy)_2(\mathbf{5H}^{\bullet})]^{2+}$, at a pH > 11.2 or pH < 11.2, respectively, the transient spectra coalesce to a single species (Figures 5). The UV−vis absorption spectra of the final transient species formed is shown in Figure 6. The absorbances attributed to both $[Ru(bpy)_2(\mathbf{5}^{\bullet-})]^{+}$ and $[Ru(bpy)_2(\mathbf{5H}^{\bullet})]^{2+}$ disappear via pH-independent second-order kinetics (Figure 7) with no significant KIE (Supporting Information, Figure S2). The rate constant of disappearance of $[Ru(bpy)_2(\mathbf{5}^{\bullet-})]^{+}$ and $[Ru(bpy)_2(\mathbf{5H}^{\bullet})]^{2+}$ is 4.5×10^8 M^{-1} s^{-1}.

Additional pulse radiolysis studies were carried out on the 90 s time scale to verify the final transient products (Figure 6, inset). At pH < 11.2, the change in absorbance over time is essentially flat, indicating that the species formed within 10 ms was indeed the final product. At pH > 11.2, there is a considerable change in absorbance indicating that the 10 ms species undergoes a further transformation on the minute time scale. Further experiments on longer time scales were, therefore, carried out using continuous radiolysis.

Continuous Radiolysis. Upon γ-irradiation (^{60}Co source) of a N_2O-saturated aqueous solution containing 10 mM $NaHCO_2$, $CO_2^{\bullet-}$ are produced in situ and continuously reduce the $[Ru(bpy)_2(\mathbf{5})]^{2+}$ compound (ca. 40 μM). A pH-dependent study of the effect of γ-irradiation was conducted to determine the products formed in relation to a constant flux of reducing radical ($CO_2^{\bullet-}$) on the minutes time scale. Since the pK_a = 11.2 was determined for the equilibrium between $[Ru(bpy)_2(\mathbf{5H}^{\bullet})]^{2+}/[Ru(bpy)_2(\mathbf{5}^{\bullet-})]^{+}$, the ^{60}Co experiments were performed at a pH of 9.1 and 13.3.

(67) Sun, H.; Hoffman, M. Z.; Mulazzani, Q. G. *Res. Chem. Int.* **1994**, *20*, 735–754.
(68) Anderson, P. A.; Anderson, R. F.; Furue, M.; Junk, P. C.; Keene, F. R.; Patterson, B. T.; Yeomans, B. D. *Inorg. Chem.* **2000**, *39*, 2721–2728.
(69) Dangelantonio, M.; Mulazzani, Q. G.; Venturi, M.; Ciano, M.; Hoffman, M. Z. *J. Phys. Chem.* **1991**, *95*, 5121–5129.
(70) Casalboni, F.; Mulazzani, Q. G.; Clark, C. D.; Hoffman, M. Z.; Orizondo, P. L.; Perkovic, M. W.; Rillema, D. P. *Inorg. Chem.* **1997**, *36*, 2252–2257.

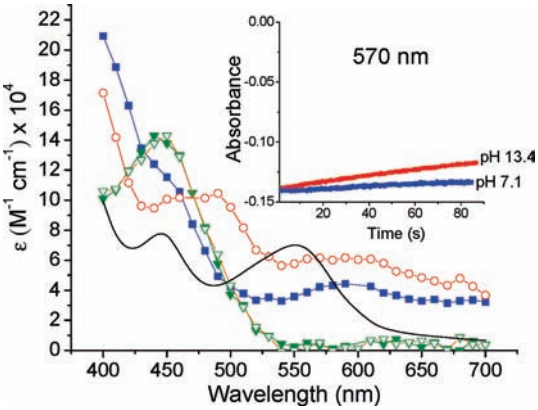

Figure 6. UV−vis absorbance spectra in H_2O at pH 7.1 and 12.5, corrected for parent compound loss assuming stoichiometric loss of $[Ru(bpy)_2(\mathbf{5})]^{2+}$ and generation of transient species (protonated radical at pH 7.1, 100 μs after pulse: squares (■); radical anion at pH 12.5, 100 μs after pulse: open circles (○); dimer at pH 7.1, 10 ms after pulse: triangles (▲); dimer at pH 12.5, 10 ms after pulse: open triangles (△); and $[Ru(bpy)_2(\mathbf{5})]^{2+}$: solid line (—)). Inset: Absorbance trace at a pH of 7.1 and 13.4 measured at 570 nm in H_2O, 90 s after pulse.

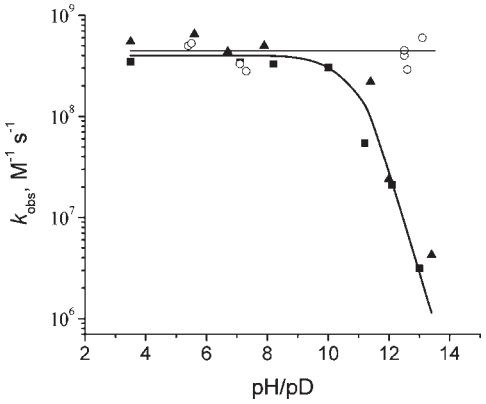

Figure 7. The pH independence of the observed second-order rate constants for the disappearance of $[Ru(bpy)_2(\mathbf{5}^{\bullet-})]^+$ and $[Ru(bpy)_2(\mathbf{5}H^{\bullet})]^{2+}$ (in H_2O = open circles, ○) compared to the pH dependence of the observed second-order rate constants for the disappearance of $[Ru(bpy)_2(pbn^{\bullet-})]^+$ and of $[Ru(bpy)_2(pbnH^{\bullet})]^{2+}$ (in H_2O = squares, ■; in D_2O = triangles, ▲). For the $[Ru(bpy)_2(\mathbf{5}^{\bullet-})]^+$ and $[Ru(bpy)_2(\mathbf{5}H^{\bullet})]^{2+}$ species, experiments in D_2O showed no difference from those performed in H_2O.

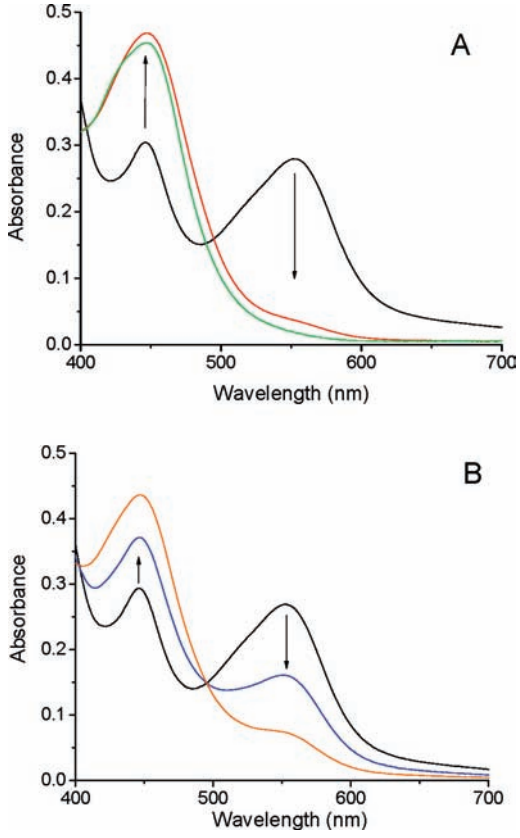

Figure 8. (A) UV−vis absorbance spectra of $[Ru(bpy)_2(\mathbf{5})]^{2+}$ after exposure to $CO_2^{\bullet-}$ from steady-state radiolysis using a ^{60}Co γ-ray source at a pH of 9.1; black t = 0 s, red t = 100 s, and green t = 220 s. (B) UV−vis absorbance spectra of $[Ru(bpy)_2(\mathbf{5})]^{2+}$ after exposure to $CO_2^{\bullet-}$ from steady-state radiolysis using a ^{60}Co γ-ray source at a pH of 13.3; black t = 0 s, blue t = 100 s, orange t = 220 s. A continuous flux of radicals is produced at a low steady-state concentration, with a production rate of ca. 0.4 μM $CO_2^{\bullet-}$/s in N_2O-saturated solutions containing HCO_2^-.

At a pH of 9.1, loss of $[Ru(bpy)_2(\mathbf{5})]^{2+}$ is accomplished in the time required to produce one equivalent of $CO_2^{\bullet-}$ per $[Ru(bpy)_2(\mathbf{5})]^{2+}$ (approximately 100 s under our conditions; Figure 8A). Further irradiation has minimal effect on the final spectrum of the species. The final spectrum is nearly identical to that obtained after the chemical reduction of $[Ru(bpy)_2(\mathbf{5})]^{2+}$ at pH < 11.2 (Supporting Information, Figure S3). Moreover, the final spectrum is also nearly identical to that of the $[Ru(bpy)_2(\mathbf{5}HH)]^{2+}$ compound prepared by photoirradiation with triethylamine (Supporting Information, Figure S3). The conversion of $[Ru(bpy)_2(\mathbf{5})]^{2+}$ to $[Ru(bpy)_2(\mathbf{5}HH)]^{2+}$ is a two-electron two-proton process, however, after the addition of one electron at a pH of 9.1, the spectrum remains unchanged, suggesting that the product formed after the addition of one equivalent of $CO_2^{\bullet-}$ at pH < 11.2 has similar electronic properties as the $[Ru(bpy)_2(\mathbf{5}HH)]^{2+}$ species.

At a pH of 13.3, after the time required to produce one equivalent of $CO_2^{\bullet-}$ per $[Ru(bpy)_2(\mathbf{5})]^{2+}$ (100 s), the conversion of the $[Ru(bpy)_2(\mathbf{5})]^{2+}$ compound is incomplete. The addition of one equivalent of $CO_2^{\bullet-}$ yields a spectrum that is identical to the sum of one-half $[Ru(bpy)_2(\mathbf{5})]^{2+}$ and one-half $[Ru(bpy)_2(\mathbf{5}HH)]^{2+}$ compounds, suggesting a disproportionation reaction through a bimolecular process (Figure 8B and Supporting Information, Figure S4).[52] Moreover, after 220 s irradiation, the final product spectrum becomes increasingly similar to the $[Ru(bpy)_2(\mathbf{5}HH)]^{2+}$ species. Complete conversion to $[Ru(bpy)_2(\mathbf{5}HH)]^{2+}$ was not observed and was likely due to the reactivity of the final product with additional reducing radical. It should be emphasized that at a pH above and below the pK_a the addition of one equivalent of $CO_2^{\bullet-}$ to $[Ru(bpy)_2(\mathbf{5})]^{2+}$ yields different products.

pH-Dependent Product Characterization. The chemical reduction of $[Ru(bpy\text{-}d_8)_2(\mathbf{5})]^{2+}$ was carried out at pH > 11.2 and pH < 11.2 to investigate the pH-dependent product formation. The deuteron−bipyridine complex was utilized to simplify the aromatic region of the ^1H NMR spectrum. All remaining resonances will be from the ligand **5** and its reduced forms. To identify the products formed, ^1H NMR, gradient 2D COSY NMR spectroscopy, and mass spectroscopy were performed. At pH > 11.2, the ^1H NMR spectrum of the two-electron two-proton reduced product is $[Ru(bpy\text{-}d_8)_2(\mathbf{5}HH)]^{2+}$. The species shows the characteristic set of doublets of the

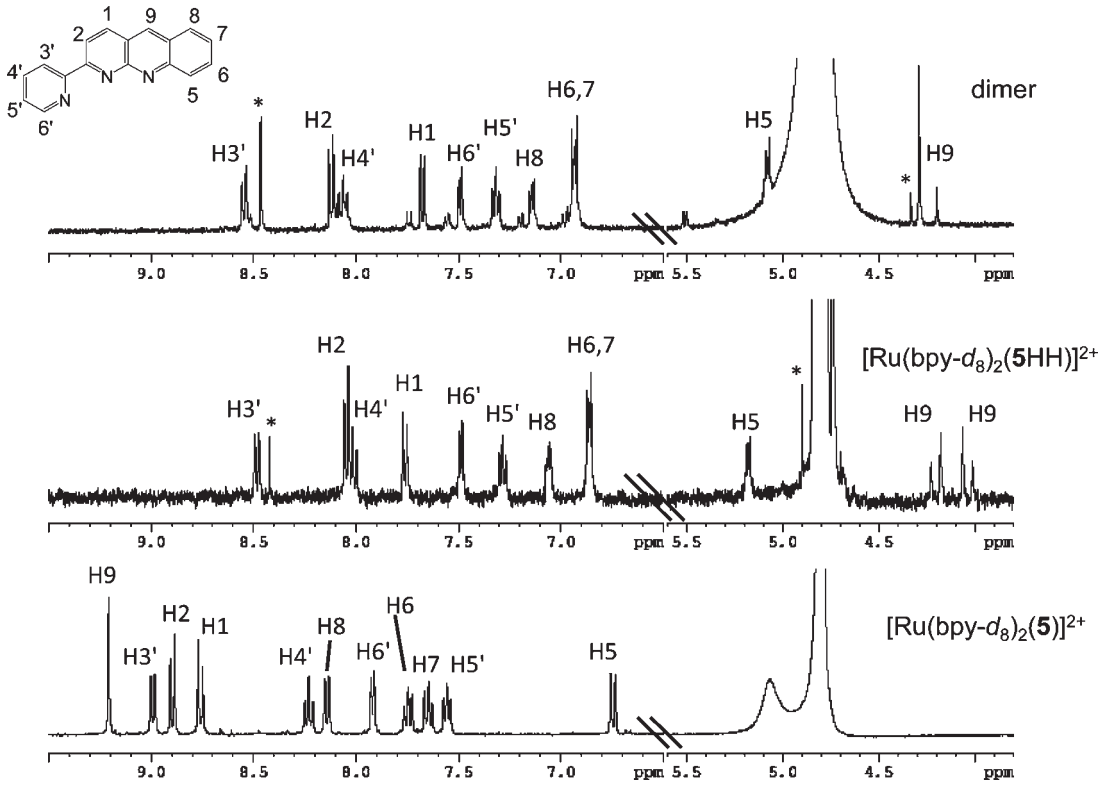

Figure 9. The ^{1}H NMR of [Ru(bpy-d_8)$_2$(**5**)]$^{2+}$ (bottom), [Ru(bpy-d_8)$_2$(**5**HH)]$^{2+}$ (middle), and [Ru(bpy-d_8)$_2$(**5**H)]$_2^{4+}$ (top) compounds in D_2O/CD_3OD. Impurities labeled (*).

inequivalent protons at 4.24 and 4.07 ppm, unequivocally identified as those that reside on the C(9) carbon (Figure 9).[52,53] The 2D COSY NMR spectrum allows for the unambiguous assignment of all the peaks in the species (Supporting Information, Figure S5). Mass spectroscopy of the sample yields m/z = 688.4 [M − (H^+, $2PF_6$)]$^+$ characteristic of the [Ru(bpy-d_8)$_2$(**5**HH)]$^{2+}$ compound.

At a pH < 11.2, the ^{1}H NMR spectrum of the product shows a spectral pattern that is more complicated than that of the [Ru(bpy-d_8)$_2$(**5**HH)]$^{2+}$ species (Figure 9). Along with the major product, a minor product is formed that exhibits resonances that are similar in place and structure as the major product. A ratio of 2:1 for the major to minor product is found. To further complicate the NMR spectrum, the D_2O solvent peak at 4.80 ppm overlaps the resonance at 5.06 ppm. Although the 5.06 ppm resonance is identifiable, 2D COSY NMR was performed to determine if any other resonances exist under the D_2O solvent peak (Supporting Information, Figure S6). No additional peaks were found to reside under the D_2O solvent peak. The singlet proton resonance at 4.29 ppm suggests that there is only one proton that resides on the C(9) carbon. This is confirmed in the 2D COSY NMR with cross-correlation peaks between the 4.29 and 7.66 ppm resonances corresponding to the proton on the C(8) or C(1) carbons. The cross-correlation and differences in peak resonances suggest that the product formed at pH < 11.2 is the dimeric species [Ru(bpy-d_8)$_2$(**5**H)]$_2^{4+}$, which contains a C−C bond between the C(9) carbons formed through dimerization of the protonated radical [Ru(bpy)$_2$(**5**H$^\bullet$)]$^{2+}$ (Figure 9). Mass spectroscopy of the reaction solution further verifies this conclusion with an m/z = 687.3 [M − ($2H^+$, $4PF_6$)]$^{2+}$.

The differences between the NMR spectra of [Ru(bpy-d_8)$_2$(**5**)]$^{2+}$, [Ru(bpy-d_8)$_2$(**5**HH)]$^{2+}$, and [Ru(bpy-d_8)$_2$(**5**H)]$_2^{4+}$ can be used to verify that starting material is not reformed during the chemical reduction and that the products formed at pH > 11.2 and pH < 11.2 are unique (Figure 9). Moreover, the NMR and mass spectroscopy results corroborate the pulse and continuous radiolysis results. At a pH < 11.2, [Ru(bpy-d_8)$_2$(**5**H)]$_2^{4+}$ is formed after the addition of one electron and one proton per [Ru(bpy-d_8)$_2$(**5**)]$^{2+}$. Additionally, the disproportionation of the [Ru(bpy-d_8)$_2$(**5**H)]$_2^{4+}$ species leads to the formation of the [Ru(bpy-d_8)$_2$(**5**HH)]$^{2+}$ compound, as seen for the reduction of the [Ru(bpy-d_8)$_2$(pbn)]$^{2+}$ species. At a pH > 11.2, [Ru(bpy-d_8)$_2$(**5**HH)]$^{2+}$ is formed after the addition of two electrons and two protons per [Ru(bpy-d_8)$_2$(**5**)]$^{2+}$.

The photochemical reactivity of the dimer species, [Ru(bpy-d_8)$_2$(**5**H)]$_2^{4+}$, was also investigated to determine the stability of the species as well as to determine if a controlled decomposition could be achieved. Photochemical irradiation of [Ru(bpy-d_8)$_2$(**5**H)]$_2^{4+}$ in a 1:1 H_2O/MeOH solution containing a trace amount of Na_2SO_4 (as an impurity) produced the [Ru(bpy-d_8)$_2$(**5**HH)]$^{2+}$ species in quantitative yield (Supporting Information, Figure S7). Photochemical irradiation in a 1:1 D_2O/CD_3OD solution produced the [Ru(bpy-d_8)$_2$(**5**HD)]$^{2+}$ species, where one hydrogen and one deuterium reside on the C(9) carbon (Supporting Information, Figure S7). However, in the dark, [Ru(bpy-d_8)$_2$(**5**H)]$_2^{4+}$ is stable under the same conditions.

Discussion

Mechanism and Product Formation of the Reduction of [Ru(bpy)$_2$(5)]$^{2+}$. In order to understand the significance of the structural change between the ligands pbn and **5**, the

Scheme 2. Mechanism for the Formation of $[Ru(bpy)_2(pbnHH)]^{2+}$

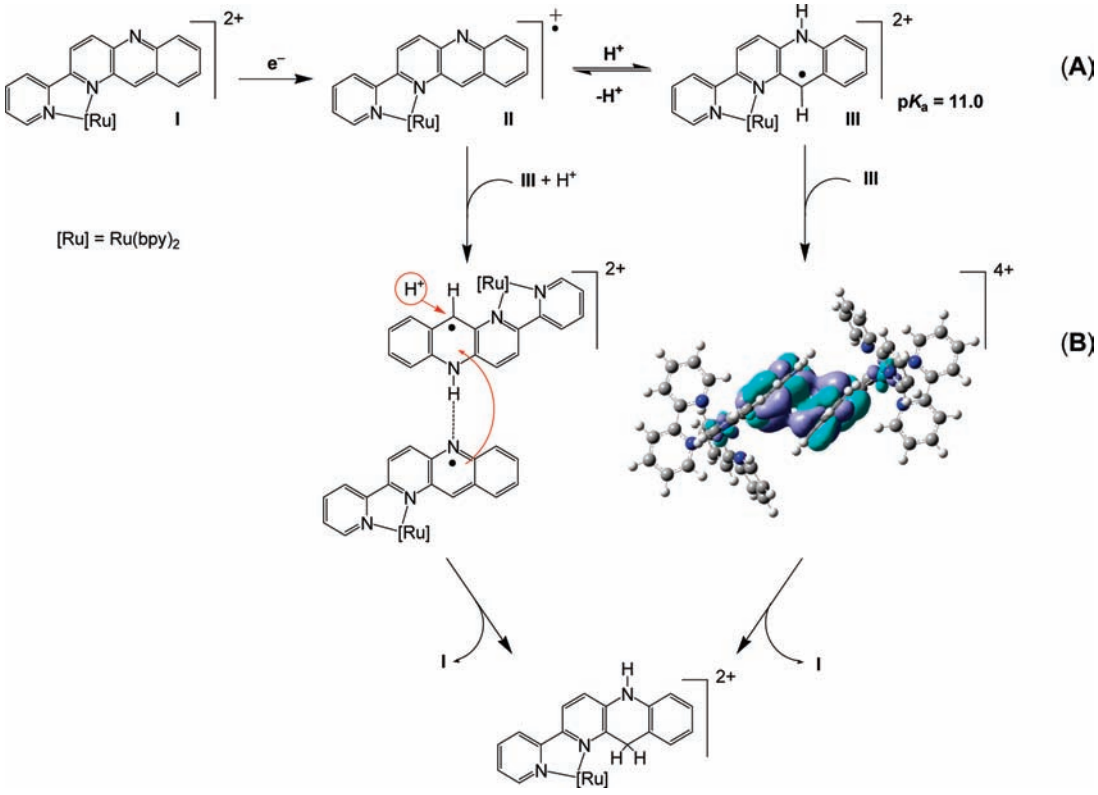

Scheme 3. pH-Dependent Mechanism of Reduction of $[Ru(bpy)_2(\mathbf{5})]^{2+}$

steps in the mechanism of formation of $[Ru(bpy)_2(pbnHH)]^{2+}$ will be compared and contrasted with those involved in the mechanism of the reduction of $[Ru(bpy)_2(\mathbf{5})]^{2+}$. The reduction of both $[Ru(bpy)_2(pbn)]^{2+}$ and $[Ru(bpy)_2(\mathbf{5})]^{2+}$ by substoichiometric pulses of $CO_2^{\bullet-}$ initially leads to the formation of the reduced anionic species $[Ru(bpy)_2(pbn^{\bullet-})]^{+}$ and $[Ru(bpy)_2(\mathbf{5}^{\bullet-})]^{+}$, respectively (Schemes 2A and 3A). The rate constant of the reaction between $CO_2^{\bullet-}$ and $[Ru(bpy)_2(pbn)]^{2+}$ is 4.6×10^9 M^{-1} s^{-1}, while those between $CO_2^{\bullet-}$ and $[Ru(bpy)_2(\mathbf{5})]^{2+}$ are 4.4×10^9 in H_2O and 3.8×10^9 M^{-1} s^{-1} in D_2O.[52] That these rate constants are indistinguishable implies that the structural difference between pbn and **5** displays a minimal effect on the initial reductions of the species in solution. Strikingly, the reduction of $[Ru(bpy)_3]^{2+}$ by $CO_2^{\bullet-}$ (6.0×10^7 M^{-1} s^{-1})[71] is 2 orders of magnitude slower than the analogous reductions for the ruthenium complexes containing ligands pbn and **5**. These differences in the reduction rate constants and the electrochemical data suggest that the pbn and **5** ligands are reduced rather than the bpy ligands. This is further supported by the very rapid reduction of ruthenium complexes containing bpz and bpm (bpz = 2,2′-bipyrazine and bpm = 2,2′-bipyrimidine) ligands by $CO_2^{\bullet-}$ (1.3×10^{10} to 4.7×10^9 M^{-1} s^{-1}), ligands that can be expected to behave similarly to pbn and **5**.[71,72]

(71) Venturi, M.; Mulazzani, Q. G.; Dangelantonio, M.; Ciano, M.; Hoffman, M. Z. *Radiat. Phys. Chem.* **1991**, *37*, 449–456.
(72) Venturi, M.; Mulazzani, Q. G.; Ciano, M.; Hoffman, M. Z. *Inorg. Chem.* **1986**, *25*, 4493–4498.

After the initial reduction by $CO_2^{\bullet-}$, protonation of the reduced anionic transients are observed for both compounds at pH < pK_a (Schemes 2A and 3A). The rate of protonation of $[Ru(bpy)_2(pbn^{\bullet-})]^+$ to $[Ru(bpy)_2(pbnH^{\bullet})]^{2+}$ is too fast to observe, but the pH-dependent change in the transient absorption spectra as well as the electrochemical data supports the proton-coupled nature of the one-electron reduced species and its conjugate acid.[52] In contrast, protonation of $[Ru(bpy)_2(\mathbf{5}^{\bullet-})]^+$ to $[Ru(bpy)_2(\mathbf{5H}^{\bullet})]^{2+}$ in H_2O can be observed, but the rate of protonation cannot be measured cleanly as the low solubility of $[Ru(bpy)_2(\mathbf{5})]^{2+}$ limits the time scale for formation of $[Ru(bpy)_2(\mathbf{5}^{\bullet-})]^+$ to slightly faster than that of the protonation process. When the reaction is carried out in D_2O, however, the rate of protonation of $[Ru(bpy)_2(\mathbf{5}^{\bullet-})]^+$ slows ($k_{2b} = 2.6 \times 10^4\ s^{-1}$) more than the rate of formation of $[Ru(bpy)_2(\mathbf{5}^{\bullet-})]^+$ at maximum solubility of the parent compound (see above) and is now measurable. An approximate KIE of 1.8 is found for the protonation of $[Ru(bpy)_2(\mathbf{5}^{\bullet-})]^+$ in D_2O/H_2O; with large error bars from the inaccuracy in measuring protonation in water. The proton source is likely the solvent (D_2O/H_2O) as protonation is independent of any general acid donor, such as phosphate or formate, and is independent of ionic strength of the solution. While very large KIEs have been observed for proton-coupled electron transfer reactions, KIEs of up to 2 have been observed for outer-sphere electron-transfer reactions or stepwise electron- and proton-transfer reactions, because of coupling with quantum modes in the solvent.[30,73−75]

As noted, the ability to observe the protonation of $[Ru(bpy)_2(\mathbf{5}^{\bullet-})]^+$ is a marked difference from the $[Ru(bpy)_2(pbn^{\bullet-})]^+$ species. While protonation of $[Ru(bpy)_2(pbn^{\bullet-})]^+$ and $[Ru(bpy)_2(\mathbf{5}^{\bullet-})]^+$ both occur on the nitrogen of their respective azaacridine ligands, the structural difference between the ligands dictate whether the protonation is slow enough to be observable. For the $[Ru(bpy)_2(pbn^{\bullet-})]^+$ species, protonation is extremely favorable and seemingly immediate due to the open accessibility of the N(10) nitrogen on the pbn ligand. In contrast, for the $[Ru(bpy)_2(\mathbf{5}^{\bullet-})]^+$ species, the protonation is inhibited due to the steric hindrance and the structural confinement of the N(10) nitrogen on the **5** ligand (Scheme 1).

As seen in previous compounds containing a ruthenium bipyridine moiety, second-order kinetics of the disappearance of the radical anionic species and its conjugate acid were determined to be consistent with a bimolecular disproportionation reaction.[52,54,69,70] The pK_a of $Ru(bpy)_2(\mathbf{5H}^{\bullet})^{2+}$ is the same as that of $Ru(bpy)_2(pbnH^{\bullet})^{2+}$. The pH dependence of the observed second-order rate constants of the disappearances of $[Ru(bpy)_2(pbn^{\bullet-})]^+$ and $[Ru(bpy)_2(pbnH^{\bullet})]^{2+}$ (Figure 7) in relation to the pH independence of the observed second-order rate constants of the disappearances of $[Ru(bpy)_2(\mathbf{5}^{\bullet-})]^+$ and $[Ru(bpy)_2(\mathbf{5H}^{\bullet})]^{2+}$ (Figure 7), however, suggests that there are distinctly different mechanisms for the overall reduction of the pbn and **5** compounds (Schemes 2B and 3B).

Previous studies in our laboratory established a mechanism for the formation of $[Ru(bpy)_2(pbnHH)]^{2+}$ in aqueous solution (Scheme 2B).[52] Below a pH of 11, two molecules of $[Ru(bpy)_2(pbnH^{\bullet})]^{2+}$ form a π-stacked dimer that is followed by a disproportionation reaction resulting in the formation of one equivalent $[Ru(bpy)_2(pbnHH)]^{2+}$ and one equivalent starting material $[Ru(bpy)_2(pbn)]^{2+}$. Further, NMR detection of the stereospecific photochemical formation of Δ-$[Ru(bpy)_2\{(S)\text{-pbn}\}]^{2+}$ and Λ-$[Ru(bpy)_2\{(R)\text{-pbn}\}]^{2+}$ in D_2O/CH_3CN indicates clear evidence of the reaction pathway via the π-stacked dimer of the deutrated one-electron reduced species.[54] The formation of the π-stacked dimer is also supported by localization of the electron in the bonding orbital between the π systems of the $[Ru(bpy)_2(pbnH^{\bullet})]^{2+}$ monomers in the calculated electronic structure of the dimer.[54] Near a pH of 11, a cross-reaction between $[Ru(bpy)_2(pbnH^{\bullet})]^{2+}$ and $[Ru(bpy)_2(pbn^{\bullet-})]^+$ leads to the formation of a hydrogen-bonded dimer.[52] The absence of a KIE indicates that disproportionation to one equivalent $[Ru(bpy)_2(pbnHH)]^{2+}$ and $[Ru(bpy)_2(pbn)]^{2+}$ may occur through electron transfer from $[Ru(bpy)_2(pbn^{\bullet-})]^+$ to $[Ru(bpy)_2(pbnH^{\bullet})]^{2+}$ followed by fast protonation of the resulting species. The reaction between two $[Ru(bpy)_2(pbn^{\bullet-})]^+$ species was determined to be negligibly small, presumably because of the lack of a proton to facilitate dimer formation.[52]

In contrast, a single pH-independent second-order rate constant ($k_{bi} = 4.5 \times 10^8\ M^{-1}\ s^{-1}$) was determined for the disappearance of both $[Ru(bpy)_2(\mathbf{5}^{\bullet-})]^+$ and $[Ru(bpy)_2(\mathbf{5H}^{\bullet})]^{2+}$ over the pH range of 5.5−13.5 (Figure 7). Coalescence of the two pH-dependent transient spectra into one spectrum over the pH range indicates that one species is formed on this time scale (tens of milliseconds) (Figure 5). Below a pH of 11, the disappearance of $[Ru(bpy)_2(\mathbf{5H}^{\bullet})]^{2+}$ is consistent with the observed bimolecular disappearance of $NAD^{\bullet}$ [37] and $NAD^{\bullet}$ analogues.[38,40,43−46,48,49] In these compounds, dimerization occurs through C−C bond formation; in the $[Ru(bpy)_2(\mathbf{5H}^{\bullet})]^{2+}$ species, the radical anion is located on the carbon trans to the N(10) nitrogen (Scheme 3B), potentially facilitating dimerization. ^{60}Co experiments confirm that only one electron per $[Ru(bpy)_2(\mathbf{5})]^{2+}$ species is required during the formation of the dimer species. Both ^1H NMR and mass spectroscopy further verify that this is the dimeric species $[Ru(bpy)_2(\mathbf{5H})]_2^{4+}$ and that disproportionation of the dimer does not readily occur in the ground state. In contrast to the pbn system, at a pH > 11, $[Ru(bpy)_2(\mathbf{5}^{\bullet-})]^+$ also undergoes a self-reaction forming the C−C bonded dimer, $[Ru(bpy)_2(\mathbf{5H})]_2^{4+}$, between the C(9) carbon anionic radicals (Figure 5 and Scheme 3B). Pulse radiolysis on the 90 s time scale confirms that $[Ru(bpy)_2(\mathbf{5H})]_2^{4+}$ is formed as an intermediate species and that it undergoes subsequent conversion to a different final product than that obtained at a pH < 11 (Figure 6 inset). The rate constant of disappearance of $[Ru(bpy)_2(\mathbf{5H})]_2^{4+}$ is approximately $3 \times 10^{-2}\ s^{-1}$. ^{60}Co experiments substantiate that the final product formed requires more than one electron per $[Ru(bpy)_2(\mathbf{5})]^{2+}$, analogous to that seen in the mechanism for reduction of $[Ru(bpy)_2(pbn)]^{2+}$. At a pH > 11, a disproportionation reaction occurs from the C−C bonded dimer forming one equivalent of hydride ($[Ru(bpy)_2(\mathbf{5HH})]^{2+}$) and one equivalent of starting material $[Ru(bpy)_2(\mathbf{5})]^{2+}$ (Supporting Information, Figure S4). Both ^1H NMR and mass spectroscopy establish that the product formed at a pH > 11.2 is $[Ru(bpy)_2(\mathbf{5HH})]^{2+}$ (Figure 9).

(73) Huynh, M. H. V.; Meyer, T. *J. Chem. Rev.* **2007**, *107*, 5004–5064.
(74) Hammes-Schiffer, S. *Acc. Chem. Res.* **2009**, *42*, 1881–1889.
(75) Yuasa, J.; Fukuzumi, S. *J. Am. Chem. Soc.* **2006**, *128*, 14281–14292.

The open accessibility of the reactive site of the $[Ru(bpy)_2(\mathbf{5}^{\bullet-})]^+$ and $[Ru(bpy)_2(\mathbf{5}H^{\bullet})]^{2+}$ species (Scheme 3) likely is responsible for the differences in mechanism and product formation with that of the reduction of the $[Ru(bpy)_2(pbn)]^{2+}$ species (Scheme 2). The pH-independent second-order rate constant (Figure 7) and coalescence of transient species in the pulse radiolysis experiments (Figure 5) indicate that on the 10 ms time scale one species is initially formed no matter the pH of the solution. At a pH < 11 in the ground state, the dimeric species $[Ru(bpy)_2(\mathbf{5}H)]_2^{4+}$ is stable on the days time scale. The NMR spectra from photolysis experiments confirm that the species is stable in the ground state, however, it disproportionates in the excited state with the proton source from H_2O/D_2O.

The C−C bonded dimer, $[Ru(bpy)_2(\mathbf{5}H)]_2^{4+}$, produced by radiation-induced reactions, disproportionates at a pH > 11. In a study to determine the stability of the dimer independently, the dimer was produced chemically at a low pH and the solution was then raised to a pH >12, the dimer decomposed to form $[Ru(bpy)_2(\mathbf{5}HH)]^{2+}$. Therefore, disproportionation of $[Ru(bpy)_2(\mathbf{5}H)]_2^{4+}$ must occur as a result of high OH^- concentration. While we do not know the first pK_a value of the dimer, a weak interaction of OH^- with the N−H protons may destabilize the dimer. Overall, rapid dimer formation and slow base-promoted disproportionation at a pH > 11 for the $[Ru(bpy)_2(\mathbf{5}^{\bullet-})]^+$ species is noteworthy because it is a significant departure from the inactivity of the $[Ru(bpy)_2(pbn^{\bullet-})]^+$ species at a high pH.[52]

Conclusion

In summary, the structural difference between $[Ru(bpy)_2(pbn)]^{2+}$ and $[Ru(bpy)_2(\mathbf{5})]^{2+}$ dictates the mechanism and the product formation in aqueous medium. Previous studies have shown that the mechanistic pathway of formation of $[Ru(bpy)_2(pbnHH)]^{2+}$ is controlled by the pH of the solution, however the hydride, $[Ru(bpy)_2(pbnHH)]^{2+}$, is formed across the entire pH range investigated.[52] Here, the exchange of the nitrogen and carbon atoms on the azaacridine ligands alters the accessibility of the reactive site, thereby changing the mechanism and the product formation for the $[Ru(bpy)_2(\mathbf{5})]^{2+}$ compound.

It was found at a pH < 11.2, protonation of the $[Ru(bpy)_2(\mathbf{5}^{\bullet-})]^+$ species is observed in D_2O with $k_{2b} = 2.6 \times 10^4$ s^{-1}. A kinetic isotope effect (KIE) of approximately 1.8 is determined for the protonation rate constants between D_2O/H_2O solutions. Dimerization of $[Ru(bpy)_2(\mathbf{5}H^{\bullet})]^{2+}$ ($k_{bi} = 4.5 \times 10^8$ M^{-1} s^{-1}) then forms the stable species $[Ru(bpy)_2(\mathbf{5}H)]_2^{4+}$. The photochemical reactivity of $[Ru(bpy\text{-}d_8)_2(\mathbf{5}H)]_2^{4+}$ was also investigated to determine the stability of the dimer species as well as to determine if a controlled decomposition could be achieved. At a pH > 11.2, following the formation of $[Ru(bpy)_2(\mathbf{5}^{\bullet-})]^+$, dimerization to $[Ru(bpy)_2(\mathbf{5}H)]_2^{4+}$ also occurs. Disproportionation of the C−C bonded dinuclear species was observed resulting in the formation of $[Ru(bpy)_2(\mathbf{5}HH)]^{2+}$ with $k_{decomp} \approx 3 \times 10^{-2}$ s^{-1}. Overall, the formation of the dimer species was found to be pH independent, while the final product formation was pH dependent for $[Ru(bpy)_2(\mathbf{5})]^{2+}$, the exact opposite of that found earlier.

In addition to the difference in the mechanism and the product formation between the $[Ru(bpy)_2(pbn)]^{2+}$ and $[Ru(bpy)_2(\mathbf{5})]^{2+}$ species, the structural difference will have a marked effect on the reactivity of the $[Ru(bpy)_2(\mathbf{5}HH)]^{2+}$ species. The reactive hydride center will be more accessible and less hindered in $[Ru(bpy)_2(\mathbf{5}HH)]^{2+}$ than in $[Ru(bpy)_2(pbnHH)]^{2+}$ (Scheme 1). Experiments to determine the ground-state hydride-donor ability of $[Ru(bpy)_2(pbnHH)]^{2+}$ and $[Ru(bpy)_2(\mathbf{5}HH)]^{2+}$ as well as the excited-state reactivity of $[Ru(bpy)_2(pbn)]^{2+}$ and $[Ru(bpy)_2(\mathbf{5})]^{2+}$ toward simultaneous electron−proton transfer reactions in CH_3CN are underway.

Acknowledgment. Work performed at BNL and University of Houston is funded under contract DE-AC02-98CH10886 and contract no. DE-FG03-02ER15334, respectively, with the U.S. Department of Energy and is supported by its Division of Chemical Sciences, Geosciences, and Biosciences, Office of Basic Energy Sciences. E.F. and D.E.C. also thank the U.S. Department of Energy for funding under the BES Solar Energy Utilization Initiative. R.P.T. thanks the Robert A. Welch Foundation (E-621).

Supporting Information Available: Synthesis and characterization of 3-(2-pyrid-2′-yl)-4-azaacridine (**5**) ligand, linear plots of observed rate constants of $[Ru(bpy)_2(\mathbf{5}^{\bullet-})]^+$ with $CO_2^{\bullet-}$ in H_2O and D_2O, plot of pH dependence of the observed second-order rate constants for disappearance of $[Ru(bpy)_2(\mathbf{5}^{\bullet-})]^+$ and $[Ru(bpy)_2(\mathbf{5}H^{\bullet})]^{2+}$, comparison of the UV−vis spectra of pH = 9.1 ^{60}Co experiment with $[(Ru(bpy)_2(\mathbf{5})]_2^{4+}$ and $[Ru(bpy)_2(\mathbf{5}HH)]^{2+}$, comparison of the UV−vis spectra of pH = 13.3 ^{60}Co experiment with the sum of half of $[(Ru(bpy)_2(\mathbf{5})]^{2+}$ and half of $[Ru(bpy)_2(\mathbf{5}HH)]^{2+}$, 2D gradient COSY of $[Ru(bpy)_2(\mathbf{5}HH)]^{2+}$, 2D gradient COSY of $[(Ru(bpy)_2(\mathbf{5}H)]_2^{4+}$, and ^1H NMR of photochemical decomposition of $[Ru(bpy\text{-}d_8)_2(\mathbf{5}H)]_2^{4+}$ in H_2O and D_2O. This material is available free of charge via the Internet at http://pubs.acs.org.